11766 *Biochemistry* **2009,** *48,* 11766–11772
DOI: 10.1021/bi9014874

BIOCHEMISTRY
including biophysical chemistry & molecular biology
Article

The IQ Domains in Neuromodulin and PEP19 Represent Two Major Functional Classes[†]

D. J. Black, David LaMartina, and Anthony Persechini*

Division of Molecular Biology and Biochemistry, University of Missouri, Kansas City, Missouri 64110-2499

Received August 25, 2009; Revised Manuscript Received October 12, 2009

ABSTRACT: The affinities of Ca^{2+}-saturated and Ca^{2+}-free calmodulin for a fluorescent reporter construct containing the PEP19 IQ domain differ by a factor of ~100, with K_d values of 11.0 ± 1.2 and 1128.4 ± 176.5 μM, respectively, while the affinities of a reporter containing the neuromodulin IQ domain are essentially identical, with K_d values of 2.9 ± 0.3 and 2.4 ± 0.3 μM, respectively. When Ca^{2+} is bound only to the C-terminal pair of Ca^{2+}-binding sites in calmodulin, the K_d value for the PEP19 reporter complex is decreased ~5-fold, while the value for the neuromodulin reporter complex is increased by the same factor. When Ca^{2+} is bound only to the N-terminal pair of Ca^{2+}-binding sites, the K_d value for the PEP19 reporter complex is unaffected, but the value for the complex with the neuromodulin reporter is increased ~12-fold. These functional differences are largely ascribed to three differences in the CaM-binding sequences of the two reporters. Replacement of a central Gly in the neuromodulin IQ domain with a Lys at this position in PEP19 almost entirely accounts for the distinctive patterns of Ca^{2+}-dependent stability changes exhibited by the two complexes. Replacement of a Lys immediately before the "IQ" amino acid pair in the neuromodulin sequence with the Ala in PEP19 accounts for the remaining Ca^{2+}-dependent differences. Replacement of an Ala in the N-terminal half of the neuromodulin sequence with the Gln in PEP19 accounts for approximately half of the Ca^{2+}-independent difference in the stabilities of the two reporter complexes, with the Ca^{2+}-independent effect of the Lys replacement accounting for most of the remainder. Since the central Gly in the neuromodulin sequence is conserved in half of all known IQ domains, these results suggest that the presence or absence of this residue defines two major functional classes.

The Ca^{2+}-binding protein calmodulin (CaM) participates at multiple levels in essentially all cellular processes. It interacts with an estimated 100 intracellular proteins, the activities of which it modulates to varying degrees with varying dependencies on the intracellular free Ca^{2+} concentration. CaM contains two pairs of EF-hand Ca^{2+}-binding domains, each comprising a globular structure that we term a "lobe". The two lobes are joined by a solvent-exposed flexible helix (*1*). Because of cooperativity within each pair of Ca^{2+}-binding sites, $(Ca^{2+})_2$CaM, with either the N-terminal or C-terminal EF-hand pair occupied, and $(Ca^{2+})_4$CaM are the major Ca^{2+}-liganded species produced (*2*). A number of proteins, including neuromodulin and PEP19, the unconventional myosins, ion channels (*3*−*5*), and modulators of small G-proteins, bind CaM through so-called "IQ domains". Depending upon their amino acid sequences, these domains can bind Ca^{2+}-free and Ca^{2+}-bound forms of CaM with quite different degrees of preference, allowing for a variety of Ca^{2+}-dependent switching behaviors (*4*).

IQ domains were first identified as light chain subunit binding sites in conventional myosins, and the consensus sequence was defined as IQxxxRGxxxR (*4*, *6*). As additional homologous domains have been discovered in other proteins, a less restricted consensus sequence has emerged: [I,L,V]QxxxR[G,x]xxx[R,K] (*4*, *6*). Structural studies demonstrate that a narrow hydrophobic cleft in the Ca^{2+}-free C-terminal CaM lobe and in the homologous regions in the myosin light chain subunits is involved in recognition of the "IQ" amino acid pair in the IQ domain (*7*−*9*). The Ca^{2+}-free N-terminal lobes in CaM and the light chains contain no such cleft, and their interactions with the IQ domain appear to be variable (*7*−*9*).

Structural and biophysical studies indicate that in the absence of Ca^{2+} there are two types of light chain or CaM complexes with IQ domains: a compact structure in which the N-terminal lobe interacts closely with the IQ domain and an extended form in which the N-terminal lobe is only weakly associated (*7*, *8*). The compact structure is formed if the semiconserved central Gly residue in the IQ consensus sequence is present, and the extended structure is formed if there is a bulky amino acid at this position (*7*, *8*). Extensive hydrophobic surfaces are exposed on both CaM lobes when they are replete with Ca^{2+}, and these appear to enfold IQ domains to form structures similar to those observed with other types of Ca^{2+}-saturated CaM complexes (*10*, *11*). Structural and biophysical studies further suggest that IQ domains adopt α-helical conformations when they are bound to Ca^{2+}-free or Ca^{2+}-saturated CaM (*7*−*11*).

The semiconserved Gly in the IQ domain consensus sequence is present in neuromodulin but has been replaced with a Lys in PEP19. The complexes between CaM and the IQ domains in these proteins are therefore expected to belong to different structural classes. To investigate the possible functional correlates of these classes, we compared the affinities of the Ca^{2+}-free, Ca^{2+}-saturated, and intermediate Ca^{2+}-bound CaM complexes with the neuromodulin and PEP19 IQ domains. Our results suggest that the IQ domains in neuromodulin and PEP19

[†]This work was supported by National Institutes of Health Grant DK53863 to A.P.

*To whom correspondence should be addressed: Division of Molecular Biology and Biochemistry, University of Missouri-Kansas City, 5007 Rockhill Rd., Kansas City, MO 64110-2499. Telephone: (816) 235-6076. Fax: (816) 235-5595. E-mail: Persechinia@umkc.edu.

 Published on Web 10/31/2009

	-4	-3	-2	-1	0	1	2	3	4	5	6	7	8	9	10	11	12	13	14	15	16	17	18	19	20
B_{IQ}	A	A	T	K	I	Q	A	A	F	R	G	H	I	T	R	K	K	L	K	D	E	K	K	G	A
$B_{IQ}K^{-1}A$	A	A	T	A	I	Q	A	A	F	R	G	H	I	T	R	K	K	L	K	D	E	K	K	G	A
$B_{IQ}A^{3}Q$	A	A	T	K	I	Q	A	Q	F	R	G	H	I	T	R	K	K	L	K	D	E	K	K	G	A
$B_{IQ}G^{6}K$	A	A	T	K	I	Q	A	A	F	R	K	H	I	T	R	K	K	L	K	D	E	K	K	G	A
B_{IQ}Tr	A	A	T	A	I	Q	A	Q	F	R	K	H	I	T	R	K	K	L	K	D	E	K	K	G	A
B_{IQ}PEP	A	A	V	A	I	Q	S	Q	F	R	K	F	Q	K	K	K	A	G	S	Q	S	-	-	-	-

FIGURE 1: Native and mutant IQ domain sequences that were investigated. The sequences listed are inserts in a previously described reporter construct that responds to CaM binding with decreases in fluorescence resonance energy transfer between two fluorescent protein variants (*12*−*14*). These decreases were monitored on the basis of the fluorescence emission at 525 nm (430 nm excitation). The aligned insert sequences are numbered in relation to the first residue (0) in the 11-residue consensus IQ motif sequence: [I,L,V]QxxxR[G, x]xxx[R,K], which is underlined. Positions −1, 3, and 6 (boxed) were the focus of these investigations. The insert sequences in B_{IQ} and B_{IQ}PEP are derived from neuromodulin and PEP19, respectively. The others were derived by replacement of amino acids in the B_{IQ} sequence with those in the B_{IQ}PEP sequence at one or all three (B_{IQ}Tr) of the indicated positions.

represent two major functional classes whose complexes with CaM each exhibit a distinctive pattern of Ca^{2+}-dependent stability changes.

MATERIALS AND METHODS

The cDNA encoding B_{IQ},[1] a fluorescent protein reporter that binds CaM via an IQ domain insert sequence derived from neuromodulin, has been described in detail elsewhere (*12*−*14*). The CaM-binding sequences in these reporter constructs are inserted between cyan and yellow variants of green fluorescence protein. When CaM is bound, the extent of fluorescence resonance transfer from the cyan donor to the yellow acceptor is decreased (*12*−*14*). The B_{IQ} reporter construct, which contains the neuromodulin IQ domain, and intact neuromodulin have previously been shown to bind CaM with similar affinities (*12*). The insert sequences in the reporter constructs we have used in these studies are listed in Figure 1. Fluorescent protein reporter constructs were expressed in *Escherichia coli* BL21(DE3) and purified as described previously (*15*). Native and mutant vertebrate CaMs were expressed in *E. coli* and purified as described in detail elsewhere (*16*, *17*). Two mutant CaMs were employed to determine the effects of Ca^{2+} binding solely to the N-terminal and C-terminal EF-hand pair: N_xCCaM (N_xC), in which Ca^{2+} ligands at positions 31 and 67 in the N-terminal EF-hand pair have been replaced with alanines, and NC_xCaM (NC_x), in which the homologous ligands at positions 104 and 140 in the C-terminal EF-hand have been replaced (*12*). We have previously determined that the mutant EF-hand pairs in these proteins do not bind Ca^{2+} under the experimental conditions used for these investigations, and that the mutant CaM lobes mimic the properties of Ca^{2+}-free native lobes (*12*).

Fluorescence Measurements. A Photon Technologies International (Monmouth Junction, NJ) QM-1 fluorometer operated in photon counting mode was used for all equilibrium fluorescence measurements. Monochromator excitation and emission slit widths were set to produce bandwidths of ∼2.5 nm. All experiments were performed at 23 °C. The standard experimental buffer contained 25 mM Tris (pH 7.5), 100 mM KCl, 100 μg/mL BSA, 25 μM TPEN, and other components as specified in the text or captions. Nominally Ca^{2+}-free conditions were produced by inclusion of 3 mM BAPTA. Saturation of functional Ca^{2+} binding sites in native or mutant CaMs was achieved via addition of $CaCl_2$ to the standard buffer and CaM stock solutions to produce a final free Ca^{2+} concentration of ∼250 μM.

Analysis of Fluorescence Data. Decreases in yellow acceptor fluorescence protein emission at 525 nm (cyan donor excited at 430 nm) due to CaM binding were used to determine fractional binding to reporter IQ domains as described in detail elsewhere (*12*). Apparent K_d values were derived from these measurements using a standard hyperbolic binding equation [FR = [CaM]/([CaM] + K_d)]. Fractional response (FR) is defined as $(F_{max} - F)/(F_{max} - F_{min})$, where F corresponds to the 525 nm fluorescence emission measured after each addition of CaM and F_{max} and F_{min} correspond to the fluorescence of the CaM-free and CaM-saturated reporter, respectively. In cases of very low-affinity interactions where F_{min} could not be approached, its value was allowed to float during fitting calculations. The F_{min} values thus obtained were not found to differ significantly from the experimental values determined for higher-affinity interactions. A hyperbolic binding equation is applicable to these data because the reporter concentrations of 15−100 nM used are at least 5-fold below the lowest CaM concentrations used. Thus, the free and total CaM concentrations can be considered to be the same. This equation describes a single-site dependence of the fractional response on CaM concentration, so the fits obtained support a 1:1 binding stoichiometry. We have previously confirmed this by performing stoichiometric titrations of the reference B_{IQ} reporter (data not shown). Reported K_d values are the means of three to five independent determinations. Errors are expressed as the standard error of the mean (SEM). The difference between two values is considered statistically significantly if the p value derived from an unpaired t-test is less than 0.05.

RESULTS

CaM Binding to B_{IQ} and B_{IQ}PEP. The first step in these investigations was to evaluate binding by B_{IQ} and B_{IQ}PEP of CaM in its four principal Ca^{2+}-liganded states, namely, Ca^{2+}-free, fully Ca^{2+}-saturated, and partially saturated, with Ca^{2+} bound only to the N-terminal (N_2CCaM) or C-terminal (NC_2CaM) EF-hand pair. Representative data are presented in Figures 2 and 3, and the K_d values derived from these and similar data are listed in Table 1. Determinations performed with B_{IQ} confirm results obtained previously with this construct (*12*). Thus, Ca^{2+}-free and Ca^{2+}-saturated CaM bind this reporter with similar K_d values of 2.4 ± 0.3 and 2.9 ± 0.3 μM, respectively. NC_2CaM and NC_2CaM are both bound more weakly, with K_d values of 12.7 ± 1.1 and 31.3 ± 2.7 μM, respectively. In contrast, B_{IQ}PEP binds Ca^{2+}-free and Ca^{2+}-saturated CaM with significantly different K_d values of 1128.4 ± 176.5 and 11.0 ± 1.2 μM, respectively, and it binds NC_2CaM and N_2CCaM with K_d values of 207.6 ± 16.5 and 988.4 ± 146.8 μM, respectively. Thus, Ca^{2+} binding to only one EF-hand pair either increases the affinity of the B_{IQ}PEP complex or has little effect, dependent upon which pair of sites is occupied.

[1]Abbreviations: B_{IQ}, fluorescent reporter containing an IQ domain sequence derived from neuromodulin; B_{IQ}PEP, fluorescent reporter containing an IQ domain sequence derived from PEP19; $B_{IQ}K^{-1}A$, $B_{IQ}A^{3}Q$, and $B_{IQ}G^{6}K$, variants of B_{IQ} with the K−1A, A3Q, and G6K substitutions, respectively; B_{IQ}Tr, variant of B_{IQ} containing all three substitutions; N_xCCaM (N_xC), mutant CaM with E31A and E67A substitutions; NC_xCaM (NC_x), mutant CaM with E104A and E140A substitutions; N_2CCaM (N_2C), CaM with Ca^{2+} bound to both N-terminal EF-hands; NC_2CaM (NC_2), CaM with Ca^{2+} bound to both C-terminal EF-hands; BAPTA, 1,2-bis(2-aminophenoxy)ethane-*N*,*N*,*N*′,*N*′-tetraacetic acid; dibromo-BAPTA, 1,2-bis(2-amino-5,5′-dibromophenoxy)ethane-*N*,*N*,*N*′,*N*′-tetraacetic acid; TPEN, tetrakis(2-pyridylmethyl)ethylenediamine.

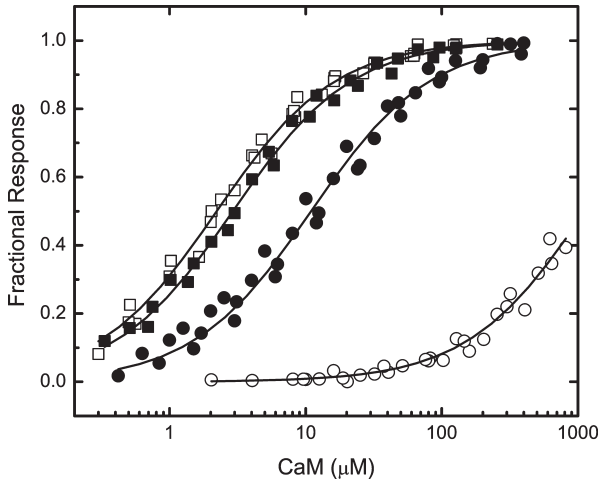

FIGURE 2: Comparison of the CaM-binding properties of reporters containing the neuromodulin and PEP19 IQ domains. Binding was evaluated on the basis of the fractional changes in the fluorescence emission of the B_{IQ} (■ and □) or B_{IQ}PEP (● and ○) reporter constructs. Binding experiments were performed in the presence of ~250 μM free Ca^{2+} (filled symbols) or 3 mM BAPTA (empty symbols). Apparent K_d values derived from fits of these (—) and similar data to a hyperbolic binding equation are listed in Table 1. Fluorescent reporter concentrations were 15−100 nM. The standard experimental buffer contained 25 mM Tris (pH 7.5), 100 mM KCl, 100 μg/mL BSA, 25 μM TPEN, and other components as specified. The fitted F_{min} value for binding of Ca^{2+}-free CaM to B_{IQ}PEP is 0.55 ± 0.07. This is not different from the value of 0.56 ± 0.07 derived for the complex of Ca^{2+}-free CaM with B_{IQ}.

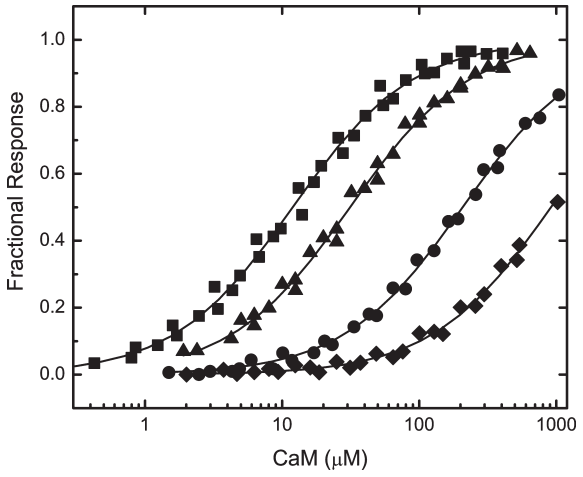

FIGURE 3: Effects of Ca^{2+} binding to the N-terminal or C-terminal EF-hand pair in CaM on its affinities for reporters containing the neuromodulin and PEP19 IQ domains. Data are presented for binding of B_{IQ} to N_xCCaM (■) or NC_xCaM (▲) and for binding of B_{IQ}PEP to N_xCCaM (●) or NC_xCaM (◆). At the free Ca^{2+} concentration of ~250 μM used for these experiments, the native EF-hand pairs in N_xCCaM and NC_xCaM are Ca^{2+}-saturated. Apparent K_d values derived from fits of a hyperbolic binding equation to these (—) and similar data are listed in Table 1. Additional experimental details are given in the legend of Figure 2. The fitted F_{min} values for binding of NC_2CaM and N_2CCaM to B_{IQ}PEP are 0.72 ± 0.03 and 0.70 ± 0.04, respectively. These are not different from the values of 0.74 ± 0.03 and 0.71 ± 0.01, respectively, derived for the complexes with B_{IQ}.

For the sake of comparison, it is preferable to express differences in the affinities of reporter complexes in terms of their stabilities instead of their K_d values, which do not scale linearly with stability. We have calculated the stability differences ($\Delta\Delta G_B$) between the CaM complexes with B_{IQ}PEP or B_{IQ} variants and the corresponding B_{IQ} complexes (Table 1). A negative $\Delta\Delta G_B$ value means that the B_{IQ}PEP or B_{IQ} variant complex is more stable than the B_{IQ} complex, while a positive value means it is less stable.

The $\Delta\Delta G_B$ values for the B_{IQ}PEP complexes with Ca^{2+}-free and Ca^{2+}-saturated CaM are 15.1 ± 2.3 and 3.3 ± 0.5 kJ/mol, respectively, and the values for the complexes with NC_2CaM and N_2CCaM are 6.9 ± 0.7 and 8.5 ± 1.5 kJ/mol, respectively. Although the B_{IQ}PEP complex is less stable overall than the B_{IQ} complex, this difference is significantly reduced when Ca^{2+} is bound to either EF-hand pair in CaM and is reduced still further when Ca^{2+} is bound to both EF-hand pairs. The two complexes therefore differ both in terms of their overall stabilities and in terms of the changes in stability produced when Ca^{2+} is bound to calmodulin.

CaM Binding to B_{IQ} Variants. As seen in Figure 1, the inserts in B_{IQ} and B_{IQ}PEP differ in length and in amino sequence at several positions. For these initial investigations, the functional significance of amino acid sequence differences at positions −1, 3, and 6 was examined. The Gly at position 6 in the neuromodulin IQ domain has been replaced with a Lys in the PEP19 sequence. Since a Gly is present at this position in approximately half of all IQ domains, we were particularly interested in the functional consequences of this replacement. The other two replacements are of interest because structural data suggest that they are likely to interact with the C-terminal CaM lobe, which plays a key role in Ca^{2+}-free CaM−IQ domain complexes (*7*−*9*). Three variants of B_{IQ} with single-amino acid replacements were generated ($B_{IQ}K^{-1}A$, $B_{IQ}A^3Q$, and $B_{IQ}G^6K$), together with one containing all three replacements (B_{IQ}Tr). The complete insert sequences for these reporter constructs are listed in Figure 1. Representative data for binding of Ca^{2+}-free and Ca^{2+}-saturated CaM, NC_2-CaM, and N_2CCaM by all of these reporters are presented in Figures 4−7. The K_d and $\Delta\Delta G_B$ values derived from these and similar data are presented in Table 1.

The $\Delta\Delta G_B$ values for the Ca^{2+}-free CaM complexes with $B_{IQ}K^{-1}A$, $B_{IQ}A^3Q$, and $B_{IQ}G^6K$ are 5.4 ± 0.9, 5.0 ± 0.7, and 2.2 ± 0.4 kJ/mol, respectively. Thus, the $K^{-1}A$ and A^3Q replacements significantly decrease the stability of the complex, while the G^6K replacement has a relatively small effect, corresponding with only a ~2-fold increase in the K_d value (Table 1). The $\Delta\Delta G_B$ values for the various Ca^{2+}-bound forms of the $B_{IQ}A^3Q$ complex are similar to the value for the Ca^{2+}-free form of this complex (Table 1). The effects of the A^3Q replacement on stability thus appear to be Ca^{2+}-independent. The $\Delta\Delta G_B$ values for the intermediate Ca^{2+}-bound forms of the $B_{IQ}K^{-1}A$ complex both appear to be less than the value of 5.4 ± 0.9 kJ/mol for the Ca^{2+}-free complex, but the differences are not quite statistically significant. The 1.3 ± 0.2 kJ/mol $\Delta\Delta G_B$ value for the Ca^{2+}-saturated form of this complex is significantly lower (Table 1). The $K^{-1}A$ replacement therefore appears to have significant Ca^{2+}-dependent and -independent effects on stability. The $\Delta\Delta G_B$ values for the complexes between $B_{IQ}G^6K$ and the Ca^{2+}-bound forms of CaM all are negative, with values ranging from -5.6 ± 0.8 to -2.2 ± 0.3 kJ/mol (Table 1), and the effects of the G^6K replacement on stability are primarily Ca^{2+}-dependent.

The $\Delta\Delta G_B$ values for the different forms of the CaM complex with B_{IQ}Tr, which contains all three amino replacements, are similar to the corresponding values for the B_{IQ}PEP complex (Table 1). The only statistically significant difference is between the values for the two NC_2CaM complexes. Thus, the combination

Table 1: K_d and $\Delta\Delta G_B$ Values for Binding of Ca^{2+}-Free and Ca^{2+}-Bound CaM[a]

	NC		NC_2[b]		N_2C[b]		N_2C_2	
construct	K_d (μM)	$\Delta\Delta G_B$ (kJ/mol)	K_d (μM)	$\Delta\Delta G_B$ (kJ/mol)	K_d (μM)	$\Delta\Delta G_B$ (kJ/mol)	K_d (μM)	$\Delta\Delta G_B$ (kJ/mol)
B_{IQ}	2.4 ± 0.3	–	12.7 ± 1.1	–	31.3 ± 2.7	–	2.9 ± 0.3	–
$B_{IQ}K^{-1}A$	21.1 ± 2.8	5.4 ± 0.9	46.6 ± 3.9	3.2 ± 0.4	118.1 ± 8.4	3.3 ± 0.4	5.0 ± 0.4	1.3 ± 0.2
$B_{IQ}A^{3}Q$	18.6 ± 1.8	5.0 ± 0.7	83.6 ± 14.0	4.6 ± 0.9	562.7 ± 60.0	7.1 ± 0.9	12.3 ± 1.1	3.6 ± 0.5
$B_{IQ}G^{6}K$	5.8 ± 0.8	2.2 ± 0.4	1.4 ± 0.2	−5.4 ± 0.8	12.7 ± 1.3	−2.2 ± 0.3	0.3 ± 0.03	−5.6 ± 0.8
sum	–	12.6 ± 1.8	–	2.4 ± 1.3	–	8.2 ± 1.0	–	−0.7 ± 1.0
B_{IQ}Tr	413.5 ± 23.4	12.7 ± 1.7	47.2 ± 4.2	3.2 ± 0.4	344.2 ± 46.1	5.9 ± 0.9	7.9 ± 0.7	2.5 ± 0.4
B_{IQ}PEP	1128.4 ± 176.5	15.1 ± 2.3	207.6 ± 16.5	6.9 ± 0.7	988.4 ± 146.8	8.5 ± 1.5	11.0 ± 1.2	3.3 ± 0.5

[a]N and C refer to the N-terminal and C-terminal EF-hand pairs in CaM, respectively, with subscripts indicating their Ca^{2+}-liganded states (2 or no Ca^{2+} bound). K_d values are given as means ± the standard error of the mean calculated from three to five individual determinations. The row labeled "sum" contains the arithmetic sums of the $\Delta\Delta G_B$ values for the B_{IQ} variants containing single-amino acid replacements.The nomenclature for IQ domain reporter constructs is defined in Figure 1. Differences in binding energy ($\Delta\Delta G_B$) were calculated according to the relationship $\Delta\Delta G_B = RT \ln[K_d(B_{IQ}N)/K_d(B_{IQ})]$, where $K_d(B_{IQ})$ is the K_d value for a Ca^{2+}-free or Ca^{2+}-bound CaM−B_{IQ} complex and $K_d(B_{IQ}N)$ is the K_d value for the corresponding complex with B_{IQ}PEP or a substituted B_{IQ} variant, as specified in the table. [b]The affinities of complexes with these Ca^{2+}-liganded states of CaM were determined in the presence of 250 μM free Ca^{2+} using N_xCCaM or NC_xCaM, which contain defective N-terminal or C-terminal EF-hand pairs, respectively, as indicated by the subscript x.

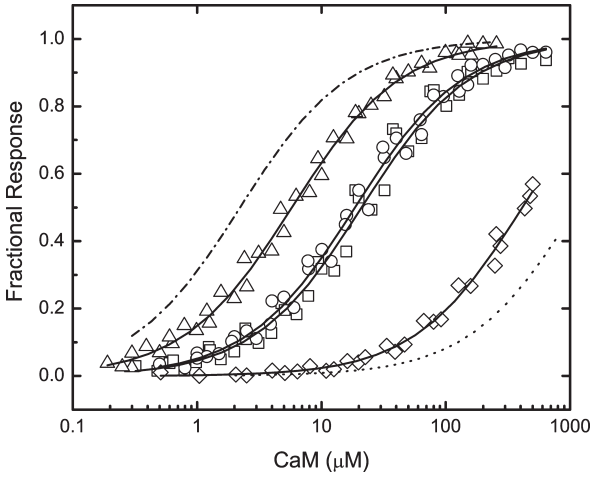

FIGURE 4: Binding of Ca^{2+}-free CaM to reporters containing mutant neuromodulin IQ domains altered to match the PEP19 sequence at positions −1, 3, and 6. Data for the following reporter constructs are presented: $B_{IQ}K^{-1}A$ (□), $B_{IQ}A^{3}Q$ (○), $B_{IQ}G^{6}K$ (△), and B_{IQ}Tr (◇), which contains all three amino acid changes. The complete amino acid sequences of the IQ domains in these reporters are listed in Figure 1. Apparent K_d values derived from fits of a hyperbolic binding equation to these (—) and similar data are listed in Table 1. Nominally Ca^{2+}-free conditions were produced by addition of 3 mM BAPTA. Additional experimental details are given in Materials and Methods or in the legend of Figure 2. Fitted curves for binding of Ca^{2+}-free CaM to B_{IQ} (−·−) and B_{IQ}PEP (···) are presented for the sake of comparison (see Figure 2). The fitted F_{min} value for B_{IQ}Tr is 0.60 ± 0.01. This is not different from the values derived for the other reporter constructs, which range from 0.57 ± 0.01 to 0.59 ± 0.01.

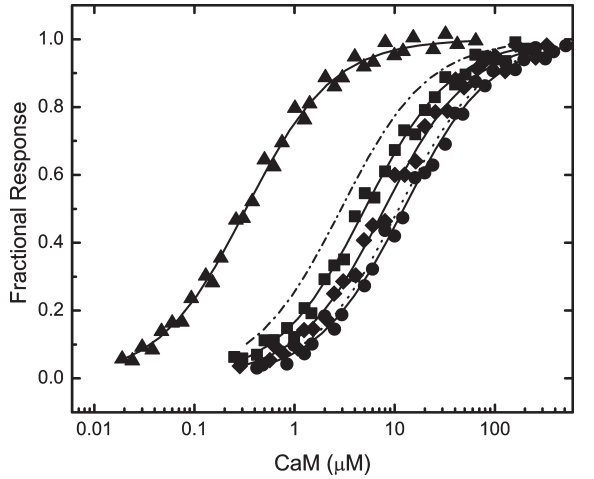

FIGURE 5: Binding of Ca^{2+}-saturated CaM to reporters containing mutant neuromodulin IQ domains altered to match the PEP19 sequence at positions −1, 3, and 6. Data for the following reporter constructs are presented: $B_{IQ}K^{-1}A$ (■), $B_{IQ}A^{3}Q$ (●), $B_{IQ}G^{6}K$ (▲), and B_{IQ}Tr (◆), which contains all three amino acid changes. The complete amino acid sequences of the IQ domains in these reporters are listed in Figure 1. Apparent K_d values derived from fits of a hyperbolic binding equation to these (—) and similar data are listed in Table 1. Ca^{2+} saturation was effected by addition of ~250 μM free Ca^{2+}. Additional experimental details are given in Materials and Methods or in the legend of Figure 2. Fitted curves for binding of Ca^{2+}-saturated CaM to B_{IQ} (−·−) and B_{IQ}PEP (···) are presented for the sake of comparison (see Figure 2).

of Ca^{2+}-independent and Ca^{2+}-dependent changes in stability produced by the three amino acid replacements appear to largely explain the functional differences between the B_{IQ} and B_{IQ}PEP complexes. The arithmetic sums of the $\Delta\Delta G_B$ values for the CaM complexes with B_{IQ} variants containing single replacements are similar to the $\Delta\Delta G_B$ values for the B_{IQ}Tr reporter complex (Table 1). The only statistically significant difference is between the two values for the Ca^{2+}-saturated complex. This additivity suggests that there is little interaction among positions −1, 3, and 6.

Energy Coupling in the CaM Complexes with B_{IQ} and B_{IQ}PEP. It is evident that Ca^{2+} binding has quite distinct effects on the stabilities of the B_{IQ} and B_{IQ}PEP complexes. To examine these differences, we have derived energy coupling ($\Delta\Delta G_C$) values for the various reporter complexes from ratios of the K_d values for the different Ca^{2+}-free and Ca^{2+}-liganded forms of CaM, as indicated in Table 2. These values define the changes in stability produced when Ca^{2+} is bound only to the C-terminal or N-terminal EF-hand pair in CaM (NC_2:NC or N_2C:NC ratio) and the changes produced when the remaining EF-hand pair is occupied (N_2C_2:NC_2 or N_2C_2:N_2C ratio). The overall effect of Ca^{2+} binding on stability is defined by the $\Delta\Delta G_C$ value derived from the N_2C_2:NC K_d ratio (Table 2). This value is, by definition, independent of whether the C-terminal (C-terminal → N-terminal binding order) or N-terminal (N-terminal → C-terminal binding order) EF-hand pair is occupied first. Although $\Delta\Delta G_C$ values could in principle be calculated from $\Delta\Delta G_B$ values, calculating them from the K_d values for a single reporter complex is preferable because it reduces the number of experimentally determined values in the calculations.

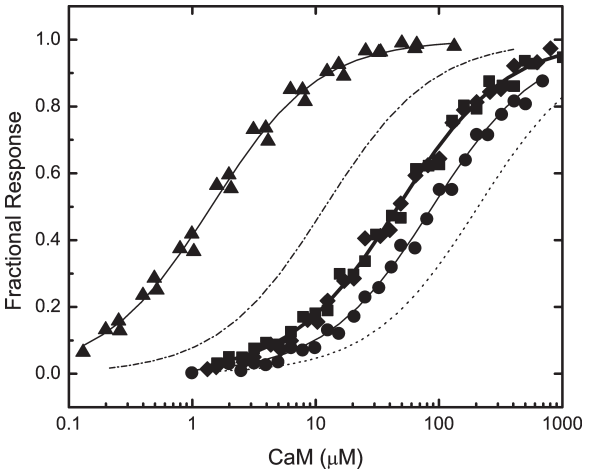

FIGURE 6: Effects of Ca^{2+} binding to the C-terminal EF-hand pair in CaM on its affinities for reporters containing mutant neuromodulin IQ domains altered to match the PEP19 sequence at positions −1, 3, and 6. Data for binding of N_xCCaM to the following reporter constructs are presented: $B_{IQ}K^{-1}A$ (■), $B_{IQ}A^3Q$ (●), $B_{IQ}G^6K$ (▲), and $B_{IQ}Tr$ (◆), which contains all three amino acid changes. The complete amino acid sequences of the IQ domains in these reporters are listed in Figure 1. At the free Ca^{2+} concentration of ~250 μM used for these experiments, the native EF-hand pair in N_xCCaM is Ca^{2+}-saturated. Apparent K_d values derived from fits of a hyperbolic binding equation to these (—) and similar data are listed in Table 1. Additional experimental details are given in Materials and Methods or in the legend of Figure 2. Fitted curves for binding of Ca^{2+}-saturated N_xCCaM to B_{IQ} (−·−) and $B_{IQ}PEP$ (···) are presented for the sake of comparison (see Figure 2).

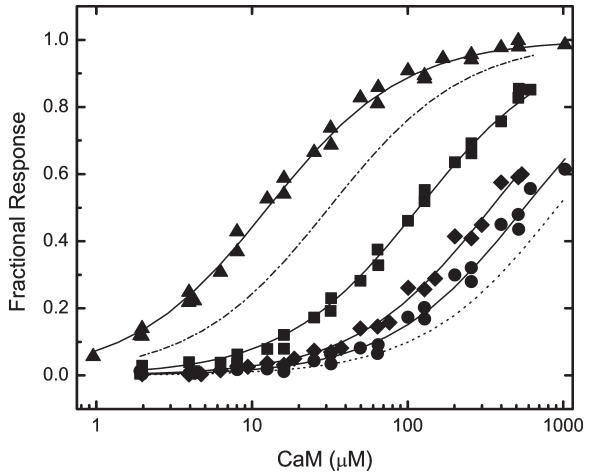

FIGURE 7: Effects of Ca^{2+} binding to the N-terminal EF-hand pair in CaM on its affinities for reporters containing mutant neuromodulin IQ domains altered to match the PEP19 sequence at positions −1, 3, and 6. Data for binding of NC_xCaM to the following reporter constructs are presented: $B_{IQ}K^{-1}A$ (■), $B_{IQ}A^3Q$ (●), $B_{IQ}G^6K$ (▲), and $B_{IQ}Tr$ (◆), which contains all three amino acid changes. The complete amino acid sequences of the IQ domains in these reporters are listed in Figure 1. At the free Ca^{2+} concentration of ~250 μM used for these experiments, the native EF-hand pair in NC_xCaM is Ca^{2+}-saturated. Apparent K_d values derived from fits of a hyperbolic binding equation to these (—) and similar data are listed in Table 1. Additional experimental details are given in Materials and Methods or in the legend of Figure 2. Fitted curves for binding of Ca^{2+}-saturated NC_xCaM to B_{IQ} (−·−) and $B_{IQ}PEP$ (···) are presented for the sake of comparison (see Figure 2). The fitted F_{min} values for $B_{IQ}A^3Q$ and $B_{IQ}Tr$ are 0.70 ± 0.03 and 0.70 ± 0.04, respectively. These are not different from the values derived for $B_{IQ}K^{-1}A$ and $B_{IQ}G^6K$, which are 0.69 ± 0.01 and 0.71 ± 0.01, respectively.

The $\Delta\Delta G_C$ values derived for the B_{IQ} and $B_{IQ}PEP$ complexes are listed in Table 2. As we have previously demonstrated (*12*), Ca^{2+} binding only to the C-terminal or N-terminal EF-hand pair in CaM lowers the stability of the B_{IQ} complex, with a $\Delta\Delta G_C$ value of 4.1 ± 0.6 or 6.5 ± 0.9 kJ/mol, respectively (Table 2). These are balanced by the $\Delta\Delta G_C$ values for Ca^{2+} binding to the unoccupied N-terminal or C-terminal EF-hand pair, which are −3.5 ± 0.5 or −5.8 ± 0.8 kJ/mol, respectively. As a result, the stabilities of the Ca^{2+}-free and Ca^{2+}-saturated complexes are essentially identical, with an overall $\Delta\Delta G_C$ value of 0.7 ± 0.1 kJ/mol. As might be inferred from its $\Delta\Delta G_B$ values, the situation with the $B_{IQ}PEP$ complex is quite different. When Ca^{2+} is bound only to the C-terminal or N-terminal EF-hand pair in CaM, the stability of this complex is increased or remains approximately the same, with $\Delta\Delta G_C$ values of −4.2 ± 0.5 and −0.5 ± 0.1 kJ/mol, respectively. In both cases, binding to the unoccupied N-terminal or C-terminal EF-hand pair increases stability, with a $\Delta\Delta G_C$ value of −6.3 ± 1.1 or −10.9 ± 2.1 kJ/mol, respectively. The overall $\Delta\Delta G_C$ value for the $B_{IQ}PEP$ complex is −11.4 ± 1.8 kJ/mol, corresponding to the ~100-fold decrease in the K_d value noted earlier (Table 2). A key aspect of this behavior is its asymmetry with respect to the order of Ca^{2+} binding: in the C-terminal → N-termina order, the overall increase in stability is distributed over both steps, while in the in N-terminal → C-terminal order, it occurs entirely at the second step.The $\Delta\Delta G_C$ values for the $B_{IQ}PEP$ complex are consistent with equilibrium Ca^{2+} binding constants reported for the CaM complex with a peptide containing the PEP19 IQ domain (*18*).

Energy Coupling in the CaM Complexes with B_{IQ} Variants. The overall $\Delta\Delta G_C$ value for the $B_{IQ}K^{-1}A$ complex is −3.5 ± 0.6 kJ/mol, which is ~4 kJ/mol less than the overall value for the B_{IQ} complex and ~8 kJ/mol larger than the overall value for the $B_{IQ}PEP$ complex (Table 2). The $\Delta\Delta G_C$ values for the individual steps in both the C-terminal → N-terminal and N-terminal → C-terminal Ca^{2+} binding orders appear to be ~2 kJ/mol lower than the values for the B_{IQ} complex. However, most of these differences are not quite statistically significant. It is therefore unclear how the $K^{-1}A$ substitution affects stability at the level of the individual Ca^{2+} binding steps, although the significant decrease in the overall $\Delta\Delta G_C$ value is apparently not produced at a single step.

The overall $\Delta\Delta G_C$ value for the $B_{IQ}G^6K$ complex is −7.0 ± 1.1 kJ/mol, which is ~8 kJ/mol lower than the overall value for the B_{IQ} complex and ~4 kJ/mol larger than the value for the $B_{IQ}PEP$ complex. The steps in the C-terminal → N-terminal Ca^{2+} binding order have $\Delta\Delta G_C$ values of −3.4 ± 0.6 and −3.6 ± 0.6 kJ/mol, respectively, while the values for the steps in the N-terminal → C-terminal order are 1.8 ± 0.3 and −8.5 ± 1.2 kJ/mol, respectively. This asymmetric pattern of Ca^{2+}-dependent stability changes closely resembles the one exhibited by the $B_{IQ}PEP$ complex (Table 2).

The overall $\Delta\Delta G_C$ value for $B_{IQ}A^3Q$ complex is identical to the value for the B_{IQ} complex (Table 2), and $\Delta\Delta G_C$ values for the individual steps in the C-terminal → N-terminal and N-terminal → C-terminal Ca^{2+} binding orders do not differ to a statistically significant degree from the values for the B_{IQ} complex (Table 2). Thus, as suggested by the $\Delta\Delta G_B$ values for this complex, the ~5 kJ/mol decrease in stability produced by the A^3Q replacement appears to be Ca^{2+}-independent.

The $\Delta\Delta G_C$ values for the $B_{IQ}Tr$ and $B_{IQ}PEP$ complexes appear to be similar, and none of the apparent differences between them are statistically significant (Table 2). Since the effect of the A^3Q

Table 2: $\Delta\Delta G_C$ Values for CaM−IQ Domain Complexes[a]

	NC_2:NC		N_2C_2:NC_2		N_2C:NC		N_2C_2:N_2C		N_2C_2:NC	
construct	K_d ratio	$\Delta\Delta G_C$ (kJ/mol)	K_d ratio	$\Delta\Delta G_C$ (kJ/mol)	K_d ratio	$\Delta\Delta G_C$ (kJ/mol)	K_d ratio	$\Delta\Delta G_C$ (kJ/mol)	K_d ratio	$\Delta\Delta G_C$ (kJ/mol)
B_{IQ}	5.4 ± 0.8	4.1 ± 0.6	0.2 ± 0.03	−3.5 ± 0.5	14.1 ± 1.9	6.5 ± 0.9	0.09 ± 0.012	−5.8 ± 0.8	1.3 ± 0.2	0.7 ± 0.1
$B_{IQ}K^{-1}A$	2.2 ± 0.4	1.9 ± 0.3	0.1 ± 0.01	−5.5 ± 0.6	5.6 ± 0.9	4.2 ± 0.7	0.04 ± 0.005	−7.8 ± 0.8	0.2 ± 0.09	−3.5 ± 0.6
$B_{IQ}A^{3}Q$	4.8 ± 1.0	3.8 ± 0.8	0.1 ± 0.03	−4.8 ± 1.1	33.3 ± 4.9	8.6 ± 1.4	0.02 ± 0.003	−9.2 ± 1.7	0.7 ± 0.08	−0.7 ± 0.2
$B_{IQ}G^{6}K$	0.2 ± 0.04	−3.4 ± 0.6	0.2 ± 0.04	−3.6 ± 0.6	1.8 ± 0.3	1.5 ± 0.3	0.03 ± 0.004	−8.5 ± 1.2	0.06 ± 0.008	−7.0 ± 1.1
B_{IQ}Tr	0.1 ± 0.02	−5.3 ± 0.7	0.2 ± 0.02	−4.4 ± 0.7	0.8 ± 0.2	−0.4 ± 0.1	0.02 ± 0.004	−9.3 ± 1.5	0.02 ± 0.002	−9.7 ± 1.2
B_{IQ}PEP	0.2 ± 0.03	−4.2 ± 0.5	0.1 ± 0.02	−6.3 ± 1.1	0.8 ± 0.2	−0.5 ± 0.1	0.01 ± 0.003	−10.9 ± 2.1	0.01 ± 0.002	−11.4 ± 1.8

[a]The indicated K_d ratios were calculated for each reporter construct from the K_d values listed in Table 1 for binding of the different Ca^{2+}-liganded forms of CaM (NC, NC_2, N_2C, or N_2C_2). Energy coupling ($\Delta\Delta G_C$) values were calculated from these K_d ratios according to the relationship $\Delta\Delta G_C = RT\ln(K_d \text{ ratio})$. A positive $\Delta\Delta G_C$ value means that Ca^{2+} binding to the indicated EF-hand pair(s) increases the K_d for the complex; a negative value means that Ca^{2+} binding decreases the K_d for the complex.

replacement on stability is Ca^{2+}-independent, the sum of the Ca^{2+}-dependent effects of the $K^{-1}A$ and $G^{6}K$ replacements must account for the distinctive patterns of Ca^{2+}-dependent stability changes exhibited by the B_{IQ} and B_{IQ}PEP complexes. Indeed, the $G^{6}K$ replacement alone appears to account for most of the differences between the two reporter complexes in this regard.

DISCUSSION

As reported previously and confirmed here, the stability of the B_{IQ} reporter complex decreases when Ca^{2+} is bound to a single EF-hand pair, but Ca^{2+} binding has little or no overall effect on stability (*12*). This produces a biphasic change in the stability of the complex as the free Ca^{2+} concentration is increased (*12*). These characteristics are shared by the CaM complex with full-length neuromodulin (*12*). In contrast, when Ca^{2+} is bound to a single EF-hand pair in the B_{IQ}PEP reporter complex, it either increases stability or has little effect, depending on whether the C-terminal or N-terminal EF-hand pair is occupied, and occupancy of both EF-hand pairs substantially increases the stability of this complex, producing an ~100-fold decrease in the K_d value. Our results indicate that a $G^{6}K$ replacement largely accounts for the distinctive patterns of intermediate and overall Ca^{2+}-dependent stability changes exhibited by the B_{IQ} and B_{IQ}PEP complexes. The $K^{-1}A$ replacement accounts for the remaining Ca^{2+}-dependent differences. This and the $A^{3}Q$ replacement account for most of the Ca^{2+}-independent differences between the two complexes.

A Gly residue is found at position 6 in approximately half all known IQ domain sequences (Figure 8), so our results suggest that the presence or absence of this residue defines two major functional classes. Consistent with this hypothesis, a variety of published data demonstrate that the identity of the amino acid at this position significantly affects the structure of a CaM−IQ domain complex.

Two Major Structural Classes of CaM−IQ Domain Complexes. Structural and biophysical studies indicate that myosin light chain subunits and Ca^{2+}-free CaM can form two different types of complexes with IQ domains. One is compact, with the N-terminal lobe interacting closely with the IQ domain, and the other extended, with the N-terminal lobe largely free of the IQ domain (*7*, *8*). Although crystal structures supporting an extended conformation have been determined only for light chain subunits bound to myosin IQ domains, fluorescence energy transfer measurements performed with labeled CaM and peptides indicate that CaM forms similar complexes with these domains (*7*, *8*). Crystal structures supporting a compact

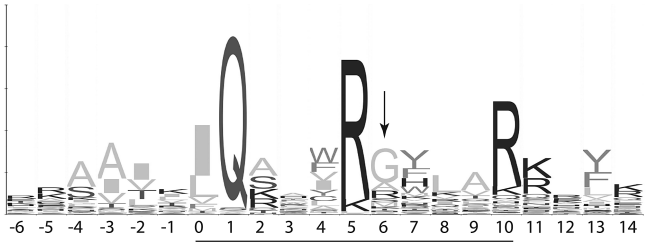

FIGURE 8: Logo representation of the aligned sequences of 3000 IQ domain regions in the Pfam-A database. The sequence is numbered in relation to the first residue (0) in the 11-residue IQ motif, which has been underlined. Each position is represented by a stack of one-letter amino acid symbols. The total height of a stack is an indication of how well conserved that position is; the height of each amino acid symbol in a stack is an indication of its relative frequency. The arrow indicates a semiconserved Gly residue that appears to be a major determinant of the pattern of Ca^{2+}-dependent stability changes exhibited by a CaM−IQ domain complex.

conformation have been determined for both CaM and light chain subunit complexes with myosin IQ domains containing the semiconserved Gly (*7*−*9*). Structural and biophysical investigations of native and specifically altered IQ domains indicate that for the compact structure to be formed Gly or another small amino acid (Ala, Ser, Thr, or Val) must be present at position 6 in the IQ domain, and a basic residue must also be present at position 10, which is well-conserved (see Figure 8). The presence of a bulky amino acid (Lys, Arg, or Met) at position 6 appears to result in the extended conformation (*7*, *8*). Structural studies suggest that the N-terminal CaM lobe interacts extensively with the IQ domain in Ca^{2+}-saturated complexes, regardless of the identity of the residue at position 6, and this is presumably also the case for the N-terminal lobes in the Ca^{2+}-saturated B_{IQ} and B_{IQ}PEP complexes (*10*, *11*). In both Ca^{2+}-free and Ca^{2+}-saturated CaM−IQ domain complexes, the C-terminal CaM lobe appears to interact with the N-terminal half of the IQ domain (*7*, *8*, *10*, *11*). This is consistent with the significant Ca^{2+}-independent effects on stability produced by the $K^{-1}A$ and $A^{3}Q$ replacements, which are in this region. The semiconserved nature of the Gly at position 6 (Figure 8) suggests that its role goes beyond allowing the compact Ca^{2+}-free CaM−IQ domain complex, since this does not appear to specifically require a Gly. We are currently investigating additional B_{IQ} variants to determine the specific functional effects of amino acid variations at this position.

Relating the Functional and Probable Structural Effects of the $G^{6}K$ Substitution. On the basis of the dissusion given above, the Ca^{2+}-free CaM complex with B_{IQ} is likely to be in

the compact conformation, while the complexes with B_{IQ}PEP and $B_{IQ}G^6K$ are likely to be in the extended conformation. Although the ~2 kJ/mol decrease in stability associated with the G^6K substitution is not entirely consistent with loss of interactions with the Ca^{2+}-free N-terminal lobe, this relatively small effect may be an underestimate of the contribution of these interactions to stability. This is because replacement of the Gly might be expected also to be stabilizing, given the probable α-helical conformation of the bound IQ domain (*7*−*9*).

When Ca^{2+} is bound only to the N-terminal EF-hand pair in CaM, it has a minimal effect on the stabilities of the B_{IQ}PEP and $B_{IQ}G^6K$ complexes, suggesting that the N-terminal lobe not only is extended in these complexes in the absence of Ca^{2+} but remains so in this Ca^{2+}-bound state. In contrast, Ca^{2+} binding only to the N-terminal EF-hand pair in the B_{IQ} complex produces an ~7 kJ/mol decrease in stability. This may reflect a loss of interactions with the N-terminal lobe when Ca^{2+} is bound and/or formation of an antagonistic interaction between the Ca^{2+}-bound N-terminal lobe and the IQ domain.

When Ca^{2+} is bound only to the C-terminal EF-hand pair in CaM, it decreases the stability of the B_{IQ} complex by ~4 kJ/mol and has the opposite effect on the B_{IQ}PEP and $B_{IQ}G^6K$ complexes (Table 2). However, the essentially identical increases in the stabilities of the all the complexes examined produced when Ca^{2+} is subsequently bound to the N-terminal EF-hand pair suggest that the N-terminal CaM lobe is in a similar state in the intermediate Ca^{2+}-bound complexes (Table 2).

Our results suggest that the presence or absence of a Gly at position 6 defines two major classes of IQ domains whose complexes with CaM exhibit distinct patterns of Ca^{2+}-dependent stability changes. This is likely to at least in part be a reflection of differences in interactions with the N-terminal CaM lobe in these two classes. Additional structural and biophysical investigations are needed to confirm and extend this hypothesis. Structures of the intermediate Ca^{2+}-bound states of CaM−IQ domain complexes are particularly important, as major differences between the stabilities of these states appear to be a key feature of the two classes.

REFERENCES

1. Persechini, A., Yano, K., and Stemmer, P. M. (2000) Ca^{2+} binding and energy coupling in the calmodulin-myosin light chain kinase complex. *J. Biol. Chem. 275*, 4199–4204.
2. Forsén, S., Vogel, H. J., and Drakenberg, T. (1986) Biophysical studies of calmodulin. In Calcium and Cell Function (Cheung, W. Y., Ed.) pp 113−157, Academic Press, New York.
3. Mooseker, M. S., and Cheney, R. E. (1995) Unconventional myosins. *Annu. Rev. Cell Dev. Biol. 11*, 633–675.
4. Jurado, L. A., Chockalingam, P. S., and Jarrett, H. W. (1999) Apocalmodulin. *Physiol. Rev. 79*, 661–682.
5. Yus-Najera, E., Santana-Castro, I., and Villarroel, A. (2002) The identification and characterization of a noncontinuous calmodulin-binding site in noninactivating voltage-dependent KCNQ potassium channels. *J. Biol. Chem. 277*, 28545–28553.
6. Bahler, M., and Rhoads, A. (2002) Calmodulin signaling via the IQ motif. *FEBS Lett. 513*, 107–113.
7. Terrak, M., Rebowski, G., Lu, R. C., Grabarek, Z., and Dominguez, R. (2005) Structure of the light chain-binding domain of myosin V. *Proc. Natl. Acad. Sci. U.S.A. 102*, 12718–12723.
8. Terrak, M., Wu, G. M., Stafford, W. F., Lu, R. C., and Dominguez, R. (2003) Two distinct myosin light chain structures are induced by specific variations within the bound IQ motifs: Functional implications. *EMBO J. 22*, 362–371.
9. Houdusse, A., Gaucher, J. F., Krementsova, E., Mui, S., Trybus, K. M., and Cohen, C. (2006) Crystal structure of apo-calmodulin bound to the first two IQ motifs of myosin V reveals essential recognition features. *Proc. Natl. Acad. Sci. U.S.A. 103*, 19326–19331.
10. Van Petegem, F., Chatelain, F. C., and Minor, D. L. (2005) Insights into voltage-gated calcium channel regulation from the structure of the Ca(V)1.2 IQ domain-Ca^{2+}/calmodulin complex. *Nat. Struct. Mol. Biol. 12*, 1108–1115.
11. Mori, M. X., Vander Kooi, C. W., Leahy, D. J., and Yue, D. T. (2008) Crystal structure of the CaV2 IQ domain in complex with Ca^{2+}/calmodulin: High-resolution mechanistic implications for channel regulation by Ca^{2+}. *Structure 16*, 607–620.
12. Black, D. J., Leonard, J., and Persechini, A. (2006) Biphasic Ca^{2+}-dependent switching in a calmodulin-IQ domain complex. *Biochemistry 45*, 6987–6995.
13. Persechini, A., and Cronk, B. (1999) The relationship between the free concentrations of Ca^{2+} and Ca^{2+}-calmodulin in intact cells. *J. Biol. Chem. 274*, 6827–6830.
14. Persechini, A., and Stemmer, P. M. (2002) Calmodulin is a limiting factor in the cell. *Trends Cardiovasc. Med. 12*, 32–37.
15. Persechini, A. (2002) Monitoring the intracellular free Ca^{2+}-calmodulin concentration with genetically-encoded fluorescent indicator proteins. *Methods Mol. Biol. 173*, 365–382.
16. Fruen, B. R., Black, D. J., Bloomquist, R. A., Bardy, J. M., Johnson, J. D., Louis, C. F., and Balog, E. M. (2003) Regulation of the RYR1 and RYR2 Ca^{2+} release channel isoforms by Ca^{2+}-insensitive mutants of calmodulin. *Biochemistry 42*, 2740–2747.
17. Tang, W., Halling, D. B., Black, D. J., Pate, P., Zhang, J. Z., Pedersen, S., Altschuld, R. A., and Hamilton, S. L. (2003) Apocalmodulin and Ca^{2+} calmodulin-binding sites on the Ca(V)1.2 channel. *Biophys. J. 85*, 1538–1547.
18. Putkey, J. A., Waxham, M. N., Gaertner, T. R., Brewer, K. J., Goldsmith, M., Kubota, Y., and Kleerekoper, Q. K. (2008) Acidic/IQ motif regulator of calmodulin. *J. Biol. Chem. 283*, 1401–1410.